



Published in final edited form as:

Anal Chem. 2013 December 3; 85(23): 11440–11448. doi:10.1021/ac402516u.

## Biochemical and Functional Characterization of Charge-defined Subfractions of High-density Lipoprotein From Normal Adults

Ju-Yi Hsieh<sup>#†</sup>, Chiz-Tzung Chang<sup>#†,‡</sup>, Max T. Huang<sup>□</sup>, Chia-Ming Chang<sup>†</sup>, Chia-Ying Chen<sup>†</sup>, Ming-Yi Shen<sup>†,‡</sup>, Hsin-Yi Liao<sup>@</sup>, Guei-Jane Wang<sup>#,Δ,▽</sup>, Chu-Huang Chen<sup>\*,†,‡,□,¶</sup>, Chao-Jung Chen<sup>\*,@,□</sup>, and Chao-Yuh Yang<sup>\*,†,‡,□,¶</sup>

<sup>†</sup>L5 Research Center, Medical Research Department, China Medical University Hospital, 2 Yude Road, North District, Taichung, 40447, Taiwan

<sup>‡</sup>College of Medicine, China Medical University, Taichung, 40402, Taiwan

<sup>□</sup>Section of Atherosclerosis and Lipoprotein Research, Department of Medicine, Baylor College of Medicine, Houston, Texas 77030, United States

<sup>#</sup>Graduate Institute of Clinical Medical Science, China Medical University, Taichung, 40402, Taiwan

<sup>@</sup>Proteomics Core Laboratory, Department of Medical Research, China Medical University Hospital, Taichung, 40402, Taiwan

<sup>Δ</sup>Department of Medical Research, China Medical University Hospital, Taichung, 40402, Taiwan

<sup>▽</sup>Department of Health and Nutrition Biotechnology, Asia University, Taichung 41354, Taiwan

<sup>¶</sup>Vascular and Medicinal Research, Texas Heart Institute, Houston, Texas 77030, United States

<sup>□</sup>Graduate Institute of Integrated Medicine, China Medical University, Taichung, 40402, Taiwan

<sup>#</sup> These authors contributed equally to this work.

### Abstract

High-density lipoprotein (HDL) is regarded as atheroprotective because it provides antioxidant and anti-inflammatory benefits and plays an important role in reverse cholesterol transport. In this paper, we outline a novel methodology for studying the heterogeneity of HDL. Using anion-exchange chromatography, we separated HDL from 6 healthy individuals into 5 subfractions (H1 through H5) with increasing charge and evaluated the composition and biologic activities of each subfraction. Sodium dodecyl sulfate polyacrylamide gel electrophoresis analysis showed that apolipoprotein (apo) AI and apoAII were present in all 5 subfractions; apoCI was present only in H1; and apoCIII and apoE were most abundantly present in H4 and H5. HDL-associated antioxidant enzymes such as lecithin-cholesterol acyltransferase, lipoprotein-associated phospholipase A<sub>2</sub>, and paraoxonase 1 were most abundant in H4 and H5. Lipoprotein isoforms were analyzed in each subfraction by using matrix-assisted laser desorption–time of flight mass spectrometry. To quantify other proteins in the HDL subfractions, we used the isobaric tags for relative and absolute quantitation approach followed by nanoflow liquid chromatography–tandem mass spectrometry analysis. Most antioxidant proteins detected were found in H4 and H5. The ability of each subfraction to induce cholesterol efflux from macrophages increased with

<sup>\*</sup>Corresponding Authors Chao-Yuh Yang, phone: 886 4 22052121 ext. 7502, chaoyuhyang@gmail.com, fax: 886-4-22077210; Chao-Jung Chen, phone: 886-4-22052121 ext. 2761, cjchen@mail.cmu.edu, fax: 886-4-22037690; and Chu-Huang Chen, phone: 832-355-9026, cchen@texasheart.org, fax: 886-355-9333..

Conflict of Interest Disclosure

The authors declare no competing financial interests.

increasing HDL electronegativity, with the exception of H5, which promoted the least efflux activity. In conclusion, anion-exchange chromatography is an attractive method for separating HDL into subfractions with distinct lipoprotein compositions and biologic activities. By comparing the properties of these subfractions, it may be possible to uncover HDL-specific proteins that play a role in disease.

## INTRODUCTION

Epidemiologic studies and prospective randomized trials have consistently shown a powerful inverse association between high-density lipoprotein (HDL) cholesterol levels and the risk of coronary heart disease; the risk is increased by approximately 3% in women and 2% in men for each 1 mg/dL decrement in HDL cholesterol level.<sup>1-3</sup> Although low plasma HDL levels have been correlated with an increased risk for cardiovascular diseases, clinical trials aimed at increasing plasma HDL levels have failed to prove any benefit, suggesting that the quality of HDL particles is more important than the quantity of total HDL.<sup>4</sup> HDL is heterogeneous, composed of 50% protein and 50% lipid by mass. The protein composition of HDL is complex and includes multiple acute-phase response proteins, protease inhibitors, and complement regulatory proteins.<sup>5-6</sup> The primary protein components of HDL are apolipoprotein (apo) AI (70%), apoAII (20%) and, to a lesser extent, apoE, clusterin (apoJ), paraoxanase (PON), haptoglobin, 2-macroglobulin, and lecithin-cholesterol acyltransferase (LCAT).<sup>7</sup> The lipid portion of HDL is composed of a phosphatidylcholine shell, a cholesteryl ester core, and small amounts of free cholesterol and triglycerides. Because of the involvement of HDL in reverse cholesterol transport (RCT)<sup>8-9</sup> and its anti-apoptotic,<sup>10</sup> anti-inflammatory, and antioxidant properties,<sup>6, 11</sup> HDL helps protect against the development of atherosclerosis.

The methodology most commonly used to separate HDL into subclasses is density-gradient ultracentrifugation, which divides whole HDL into subclasses with increasing density, known as HDL2 and HDL3.<sup>12-13</sup> In a prospective study, HDL2 showed a stronger inverse association with ischemic heart disease risk than did HDL3.<sup>12</sup> In addition, Salonen and colleagues<sup>14</sup> reported that levels of both HDL2 and total HDL were inversely associated with the risk of acute myocardial infarction, suggesting that these forms of HDL may play a protective role in ischemic heart disease. The role of HDL3 remains equivocal, although small, dense HDL3 has been shown to protect low-density lipoprotein (LDL) from oxidative stress.<sup>4, 15</sup> HDL has also been separated by using immunoaffinity chromatography and classified into 2 types of apoAI-containing lipoprotein: apoAI-containing lipoprotein with apoAII (LpA-I:A-II) and apoAI-containing lipoprotein without apoAII (LpA-I).<sup>16-17</sup> Nuclear magnetic resonance spectroscopy has been used to characterize HDL with small, medium, and large particle sizes.<sup>18</sup> In addition, pre- $\beta$  and  $\alpha$  forms of HDL have been characterized according to their electrophoretic mobility and particle size by using 2-dimensional electrophoresis.<sup>19</sup>

In several studies, researchers have reported the separation of HDL, LDL, or very-low density lipoprotein (VLDL) by using anion exchange chromatography.<sup>20-22</sup> HDL separated by using anion-exchange chromatography has been subclassified into 2 or 3 subfractions.<sup>23,24</sup> We previously used anion-exchange chromatography to separate LDL into subfractions according to charge and found that the most electronegative LDL subfraction (L5) from diabetic and hypercholesterolemic patients exhibits anti-proliferative and pro-apoptotic properties in vascular endothelial cells.<sup>25-26</sup> In the current study, we present a novel methodology for studying the heterogeneity of HDL. We used anion-exchange chromatography to separate HDL into 5 subfractions ranging from the most electropositive (H1) to the most electronegative (H5). Then, we compared each subfraction according to

lipoprotein profile and composition, the presence of functional antioxidant enzymes, and the ability to induce efflux of cholesterol from macrophages.

## EXPERIMENTAL SECTION

### Study Participants

This study was conducted according to the regulations of the China Medical University Hospital review board. Informed consent was obtained from each participant. Our study included 6 healthy participants including 2 women and 4 men (age, 25-47 years). Venous blood was collected from each participant the morning after fasting and was anticoagulated in sodium citrate (19.2 mM) or EDTA-vacutainer tubes. All participants had normal lipid values, which included total cholesterol values of 200 mg/dL, triglycerides 160 mg/dL, and LDL cholesterol 130 mg/dL.<sup>27</sup> None of the participants had systemic disease such as diabetes, hypertension, or hyperlipidemia or had a history of smoking.

### HDL Preparation

Immediately after plasma collection, the following reagents were added to the plasma to prevent oxidation and degradation in vitro: cocktail protease inhibitor (Roche Applied Sciences, Indianapolis, IN), 1% penicillin-streptomycin-neomycin-antibiotic mixture (Gibco, Life Technologies, Long Island, NY), sodium azide ( $\text{NaN}_3$ , 0.02% wt/vol), 10 mM  $\text{Na}_4\text{P}_2\text{O}_7$ , 1 mM  $\text{Na}_3\text{VO}_4$ , and 10 mM  $\beta$ -glycerophosphate. HDL was isolated from plasma by using sequential ultracentrifugation (density=1.063-1.21 g/mL).<sup>28</sup> Purified HDL was dialyzed against degassed 20 mM Tris-HCl, 0.5 mM EDTA, and 0.02%  $\text{NaN}_3$ , pH 8.0 at 4°C with 3 buffer changes in 36 hours.

### HDL Fractionation

HDL subfractions were separated by using anion-exchange columns (UnoQ12, BioRad, Hercules, CA) with an ÄKTA fast protein liquid chromatography (FPLC) system (GE Healthcare, Pittsburgh, PA), as previously described.<sup>25</sup> The columns were pre-equilibrated with buffer A (20 mM Tris-HCl, 0.5 mM EDTA, pH 8.0) in a 4°C cold room. The EDTA-containing Tris-HCl buffer was degassed before use in chromatography experiments. Up to 100 mg of HDL (10 mg/mL) was loaded onto the UnoQ12 column and separated by using a multistep gradient of buffer B (1 M NaCl in buffer A). The following buffer B gradient profile was used for the separation of HDL: isocratic at 0% for 10 minutes, 0% to 15% for 10 minutes, 15% to 20% for 30 minutes, isocratic at 20% for 10 minutes, 20% to 40% for 25 minutes, 40% to 100% for 10 minutes, isocratic at 100% for 10 minutes, and then 0% for 5 minutes. Fractions of 4 mL were collected at a flow rate of 2 mL/minute. The eluates were monitored at 280 nm and pooled into 5 subfractions, designated as H1 through H5. H1 was eluted at 18 to 28 minutes, H2 was eluted at 28 to 32 minutes, H3 was eluted at 32 to 48 minutes, H4 was eluted at 48 to 60 minutes, and H5 was eluted at 60 to 80 minutes. Each subfraction was concentrated by using Centriprep filters (YM-30, EMD Millipore, Billerica, MA) and was sterilized by being passed through a 0.20- $\mu\text{m}$  filter. The isolated fractions were stored at 4°C until further analysis was performed.

### Analysis of Lipid and Total Protein Content

We determined the distribution of phospholipids, triglycerides, free cholesterol, and total cholesterol in each HDL subfraction by using a microplate reader (Tecan Infinite M1000, Switzerland) and commercial enzymatic assay kits (Diagnostic Systems, Germany). The total protein concentration was quantified by using a bicinchoninic acid protein assay reagent kit (Thermo Scientific Pierce, Rockford, IL).<sup>29</sup> The mass of cholesteryl ester was calculated by subtracting the mass of free cholesterol from the mass of total cholesterol. The

total lipoprotein mass was calculated as the sum of the masses of total proteins, phospholipids, triglycerides, and total cholesterol. The relative percentage of each chemical constituent was then determined as the ratio of the component mass to the total lipoprotein mass.

### **Agarose Gel Electrophoresis and Sodium Dodecyl Sulfate Polyacrylamide Gel Electrophoresis (SDS-PAGE)**

HDL and HDL subfractions (2.5  $\mu\text{g}$  in 9  $\mu\text{L}$ ) were analyzed by using gel electrophoresis in 0.7% agarose (90 mM Tris and 90 mM boric acid, pH 8.2) at 100 V for 1.4 hours, as previously described.<sup>25</sup> The relative electrophoretic mobility for each subfraction was calculated as the ratio of the migration distance of the respective subfraction to that of unfractionated HDL. For SDS-PAGE analysis, HDL subfractions were delipidated with ethyl acetate:ethanol (1:1), solubilized with 10% SDS, and separated on 4-12% NuPAGE® Bis-Tris gels (Invitrogen, Carlsbad, CA) at room temperature at 55 mA for 65 min. Standards were obtained from Academy Bio-Medical Co (Houston, TX). The gels were stained for 1 hour in SimplyBlue (Invitrogen) and destained in water.

### **Matrix-assisted Laser Desorption–Time of Flight Mass Spectrometry (MALDI-TOF MS) Analysis**

Samples were prepared by depositing 1  $\mu\text{L}$  of each subfraction (H1 through H5) on the MALDI sample plate and then overlaying the sample spot with 1  $\mu\text{L}$  of saturated sinapinic acid matrix solution (30% acetonitrile/0.1% trifluoroacetic acid). Samples were then air dried. All mass spectra were obtained by using a MALDI-TOF-MS (Ultraflex III TOF/TOF, Bruker Daltonics, Germany) equipped with a smart beam laser system. To enhance sensitivity, a polydimethylsiloxane-coated MALDI plate was used.<sup>30</sup> The MALDI-TOF-MS was calibrated in the mass range of 5000–44000 m/z by using protein calibration standard 1 and 2 kits (Bruker Daltonics) containing insulin [ $\text{M}+\text{H}^+$ , 5734.52 m/z], ubiquitin I [ $\text{M}+\text{H}^+$ , 8565.76 m/z], cytochrome c [ $\text{M}+2\text{H}^{2+}$ , 6181.05 m/z;  $\text{M}+\text{H}^+$ , 12360.97 m/z], myoglobin [ $\text{M}+2\text{H}^{2+}$ , 8476.66 m/z;  $\text{M}+\text{H}^+$ , 16952.31 m/z], protein A [ $\text{M}+2\text{H}^{2+}$ , 22307.0 m/z], and trypsinogen [ $\text{M}+\text{H}^+$ , 23982.0 m/z]. MS spectra were acquired in linear mode by using a 25-kV ion source 1 voltage, a 23.45-kV ion source 2 voltage, and a pulsed anion-extraction time of 100 ns. Each mass spectrum was obtained by accumulating data from 1500-2000 laser shots.

### **Western Blot Analysis**

To determine levels of the functional proteins PON1, lipoprotein-associated phospholipase A<sub>2</sub> (Lp-PLA<sub>2</sub>), and LCAT, HDL subfractions H1 through H5 were separated by using 7.5% (LCAT and PON1; 7.5  $\mu\text{g}/\text{well}$ ) or 12% (Lp-PLA<sub>2</sub>; 35  $\mu\text{g}/\text{well}$ ) SDS-PAGE gels. Subsequently, the gels were transferred to polyvinylidenedifluoride (PVDF) membranes (BioRad), and the blots were blocked with Tris-buffered saline containing 0.1% Tween-20 and 5% (wt/vol) nonfat dry milk. Membranes were incubated with a monoclonal antibody against LCAT or PON1 (1:1000 dilution; GeneTex, Irvine, CA) or with a polyclonal antibody against Lp-PLA<sub>2</sub> (1:1000 dilution; Cayman Chemical, Ann Arbor, MI) overnight at 4°C. Membranes were then incubated with anti-rabbit secondary antibody (1:5000 dilution, GenTex) for 1 hour at room temperature. Finally, blots were developed with enhanced chemiluminescence reagents (Millipore) and analyzed with the G-box imaging system (Syngene, Cambridge, UK).

### **Determination of LCAT Activity**

The LCAT activity of each HDL subfraction was determined by using the LCAT activity assay kit (Merck, Whitehouse Station, NJ). Each HDL subfraction (10  $\mu\text{g}$ ) was incubated

with a fluorescent substrate analog in assay buffer (150 mM NaCl, 10 mM Tris-HCl, 1 mM EDTA, and 4 mM  $\beta$ -mercaptoethanol, pH 7.4) at 37°C. The conversion of nonhydrolyzed substrate (emission wavelength=470 nm) to the hydrolyzed form (emission wavelength=390 nm) was detected by using a microplate reader (Tecan Infinite M1000) at an excitation wavelength of 340 nm. The LCAT activity was calculated by measuring change in the fluorescence intensity ratio (470/390 nm) per minute.

### Determination of Antioxidant Activity

To evaluate the antioxidant activity of each HDL subfraction, we used a fluorescence assay previously described by Cominacini and colleagues.<sup>31</sup> The lag phase (initiation period) and propagation phase were both influenced by oxidant. Because the lag phase has a minor contribution to fluorescence, and the propagation phase has a major contribution to fluorescence with a significant rising rate, we used the propagation rate to determine the antioxidant activities in HDL subfractions, as previously reported by Kontush and colleagues.<sup>15</sup> LDL (20  $\mu$ g) was incubated with an HDL subfraction (40  $\mu$ g) and 10 mM 2,2'-azobis-(2-amidinopropane) hydrochloride (AAPH) at 37°C. A class of LDL peroxidation products was continuously monitored for 16 hours by using a microplate reader (Tecan Infinite M1000) set at a fluorescence wavelength of 430 nm and an excitation wavelength of 360 nm.<sup>31</sup> The propagation rates of lipid peroxidation were calculated as the increments in fluorescence value per hour at propagation phase, and maximum rates of fluorescence production were determined as the maximum value of the propagation rates.

### HDL-induced Cholesterol Efflux

To evaluate the ability of subfractions H1 through H5 to promote cholesterol efflux from macrophages, we used a method recently developed by Sankaranarayanan and colleagues.<sup>32</sup> In our study, boron-dipyrromethene (BODIPY)-cholesterol was replaced with 22-(N-(7-nitrobenz-2-oxa-1,3-diazol-4-yl)amino)-23,24-bisnor-5-cholen-3 $\beta$ -ol (22-NBD-cholesterol) (Invitrogen), a fluorescent analogue of cholesterol. RAW 264.7 cells were grown in 6-well plates with Dulbecco's modified Eagle's medium supplemented with 10% fetal bovine serum, glutamine (2 mM), penicillin (100 units/mL), and streptomycin (100  $\mu$ g/mL) in a gassed, humidified incubator (5% CO<sub>2</sub> at 37°C) until they reached 80% confluency. RAW264.7 cells were incubated for 24 hours with 5  $\mu$ g/mL 22-NBD-cholesterol. The cells were then washed and incubated for 12 hours in culture medium containing 0.2% fatty acid-free bovine serum albumin (Sigma-Aldrich, St. Louis, MO) and 0.3 mM cyclic adenosine monophosphate (Roche Applied Science). Cells in the reference wells, which provided baseline (time 0) values for total 22-NBD-cholesterol content, were lysed by using the mammalian cell lysis kit (Sigma-Aldrich). Cells in the remaining wells were incubated for 4 hours with or without HDL subfractions (10  $\mu$ g/mL). Cellular cholesterol efflux was quantified by measuring the release of cellular 22-NBD-cholesterol into the medium as a function of time. Fluorescence of the medium was measured with a microplate reader (Tecan Infinite M1000) set at 470 nm (excitation) and 530 nm (emission). The percentage of cholesterol efflux was calculated by the ratio of fluorescence intensity in the medium to the total fluorescence intensity in the cells at time 0.

### Statistical Analysis

Data are expressed as the mean  $\pm$  SD for the composition percentages, LCAT and antioxidant activities, and cholesterol efflux percentages. For the comparison of composition percentages and LCAT and antioxidant activities, significant differences were determined by using a one-way analysis of variance test with the Student-Newman-Keuls post hoc test for multiple group comparisons (SPSS version 19.0). The Student *t* test was used to compare cholesterol efflux activity. A value of  $P < 0.05$  was considered statistically significant.



## RESULTS AND DISCUSSION

### Separation of HDL into 5 Distinctive Subfractions According to Charge

Freshly prepared HDL from 6 normolipidemic study participants was separated according to ionic strength into 5 subfractions, designated as H1 through H5 (Figure 1A). H1, the most electropositive HDL subfraction, was eluted from the anion-exchange column at 18 to 28 minutes. H2, the shoulder of the largest peak, was eluted at 28 to 32 minutes. H3, the remnant of H2, was eluted at 32 to 48 minutes. H4 was eluted from isocratic elution at 48 to 60 minutes. H5, the most electronegative HDL, was eluted by incrementally increasing buffer B from 20% to 100% at 60 to 80 minutes. The subfractions of HDL showed different distributions (Figure 1A and Table 1). The H1 subfraction comprised more than half of the total HDL, and H5, which had the most electronegative characteristics, comprised only a small percentage of the total HDL.

To compare the charge of HDL subfractions, we analyzed the electrophoretic mobility of H1 through H5 (Figure 1B). H5 migrated closest to the anode, indicating that H5 was the most negatively charged subfraction. In addition, the relative electrophoretic mobility increased from subfractions H1 to H5; the relative electrophoretic mobilities of subfractions H1 through H5 were  $1.00\pm 0.04$ ,  $1.05\pm 0.06$ ,  $1.08\pm 0.05$ ,  $1.09\pm 0.06$ , and  $1.13\pm 0.03$ , respectively. These findings confirmed the increasingly negative charge of the HDL subfractions.

### Comparison of Lipid and Total Protein Content in HDL Subfractions

Table 1 lists the mean percentage values of total protein, phospholipids, triglycerides, cholesteryl ester, and total cholesterol for each of the 5 HDL subfractions. The distribution of total protein, phospholipids, free cholesterol, cholesterol ester, and total cholesterol was similar among the subfractions, whereas the percentage of triglyceride was increased in the more electronegative fractions (H3 through H5).

### SDS-PAGE Analysis of Lipoprotein Composition in HDL Subfractions

To compare the apolipoprotein composition of HDL subfractions, we subjected H1 through H5 to SDS-PAGE analysis (Figure 2). ApoCI was observed only in H1, and apoCIII was seen primarily in H5. In addition, we observed high levels of apoAI in subfractions H1 through H5. Although apoAI and apoAII were present in all 5 subfractions, the amount of these proteins slightly decreased from H1 to H5. ApoAI is the most abundant protein in HDL and is the primary structural apolipoprotein responsible for lipid metabolism. ApoAI levels have been shown to positively correlate with the ability to induce cholesterol efflux.<sup>33-34</sup> In addition, apoAI also acts as an antioxidant. When apoAI reduces lipid hydroperoxide, its Met-112 and Met-148 residues become oxidized.<sup>35</sup> The high levels of apoAI in subfractions H1 through H5 that we observed in the present study could be attributed to the diverse apoAI isoforms with post-translational modifications, such as maturity, oxidation, glycation, and carbonylation, which can modify protein size or charge.<sup>36-37</sup>

Our SDS-PAGE results also showed that apoE levels gradually increased from H1 to H5 (Figure 2). ApoE is synthesized by the liver, intestines, macrophages, and nerve cells and is recognized by the LDL receptor and the LDL receptor-related protein (LRP).<sup>38</sup> A higher apoE level in HDL is associated with decreased hepatic lipase displacement and may affect vascular triglyceride hydrolysis,<sup>39</sup> which may account for the increased levels of triglyceride we observed in subfractions H3 through H5.

## MALDI-TOF-MS Profiling of Lipoprotein Isoforms in HDL Subfractions

To identify the major apolipoproteins and their isoforms in each HDL subfraction, we used MALDI-TOF-MS, which is known for its high sensitivity, specificity, and resolution. Figure 3 shows the MS peaks for each HDL subfraction, and the apolipoprotein isoforms are labeled according to a previous study by Bondarenko and colleagues.<sup>40</sup> In the H1 subfraction, the major peaks represented apoCI isoforms, but we also detected apoAI isoforms and isoform 4 of serum amyloid A (SAA4). In the H2 subfraction, we detected apoAI, apoAII, and apoCI isoforms, as well as pro-apoCII and apoCIII<sub>1</sub>. In the H3 subfraction, we detected apoAI, apoAII, apoCI, and apoCIII isoforms and pro-apoCII. Finally, in the H4 and H5 subfractions, we detected apoCII and apoCIII isoforms; the apoCIII isoforms were the major peaks observed in the H5 subfraction.

In agreement with our SDS-PAGE results, our MALDI-TOF-MS data indicated that apoCI is found primarily in H1. Because apoCI is a low-molecular-weight, lysine-rich apolipoprotein,<sup>41</sup> we expected this protein to be electropositive and present primarily in H1. The apoCI in HDL is able to inhibit cholesteryl ester transfer protein and potentially regulate several lipase enzymes.<sup>41</sup> ApoCI', which we found primarily in H1, is a truncated apoCI isoform that lacks Thr-Pro residues at the N terminus. Dipeptidylpeptidase IV (DPPase) is thought to be responsible for truncating apoCI *in vivo*.<sup>42</sup> Reduced DPPase activity has been reported in individuals with diabetes,<sup>43</sup> and apoCI truncation was found to be decreased in an individual with hyperlipidemia.<sup>42</sup> Recently, new full (apoCI<sub>1</sub>, 6721.6 Da) and truncated (apoCI' <sub>1</sub>, 6520.0 Da) isoforms of apoCI were detected in a cohort of patients with cardiovascular disease; each isoform had a mass 90 Da higher than the respective apoCI (6631 Da) and apoCI' (6432 Da) isoforms.<sup>44</sup> These new apoCI isoforms (apoCI<sub>1</sub> and apoCI' <sub>1</sub>) were also found to be oxidized in some patients with cardiovascular disease. In a previous study, we found that oxidized apoCI and its truncated form (apoCI') are specifically detectable in patients with carotid atherosclerosis or ischemic stroke.<sup>45</sup>

Consistent with our SDS-PAGE analysis, our MALDI-TOF-MS results showed that apoCIII isoforms were detected primarily in H4 and H5. ApoCIII has 3 sialylation isoforms, designated as apoCIII<sub>0</sub>, apoCIII<sub>1</sub>, and apoCIII<sub>2</sub> according to the number of sialic acids at the Thr-74 residue. These isoforms account for 14% (apoCIII<sub>0</sub>), 59% (apoCIII<sub>1</sub>), and 27% (apoCIII<sub>2</sub>) of the apoCIII circulating in plasma.<sup>46</sup> After HDL is separated into subfractions by using anion exchange chromatography, ion suppression on MALDI-TOF-MS is greatly alleviated, which improves protein isoform detection. In addition to the detection of apoCIII isoforms in H4 and H5, we also detected a strong signal for a glycosylated form of apoCIII<sub>0</sub> (C-III<sub>0</sub>, Glyc': Galβ1, 3GalNAc-O-apoCIII<sub>0</sub>) in H5 (Figure 3). ApoCIII is synthesized primarily in the liver, similar to other apolipoproteins, and regulates apoB-containing lipoproteins by inhibiting their uptake through the LDL receptor and LRP.<sup>47-48</sup> ApoCIII can inhibit lipolysis by lipoprotein lipase and hepatic lipase, thereby impairing the uptake of triglycerides and reducing the clearance of apoB-containing lipoproteins. Thus, apoCIII plays an important role in regulating the metabolism of triglyceride-rich lipoproteins and is highly associated with hypertriglyceridemia and the progression of cardiovascular disease.<sup>49</sup> In our study, the high triglyceride levels in subfraction H3 through H5 may be attributed to the finding that apoCIII was more prevalent in the more negatively charged subfractions, which would presumably result in the increased inhibition of lipase lipolysis reactions.<sup>50</sup>

Although apoAI was detected in H1 to H5 by using SDS-PAGE, it was not detected in H4 and H5 by using MALDI-TOF-MS. One of the possible reasons for this difference may be attributed to an increase in the negatively-charged post-translational modification of apoAI in H4 and H5, such as glycation, which reduces ionization efficiency in positive mode and results in a great decrease in detection sensitivity.

Finally, our MALDI-TOF-MS results showed the detection of SAA4, an isoform of the acute-phase protein SAA. Previously, MALDI-TOF-MS was used to show that levels of the isoforms SAA1 and SAA2 increase in patients with inflammation up to 1000-fold from basal concentrations of ~1-5 mg/L.<sup>51</sup> We have also detected SAA1 and SAA2 in the HDL and plasma of patients with inflammation-related disease (unpublished data). Because the HDL samples used in our study were from healthy subjects, we detected a weak peak signal only for SAA4. The detection of SAA4 in the HDL of healthy individuals has also been reported by Farwig and colleagues.<sup>52</sup>

### Analysis of Antioxidant Enzymes in HDL Subfractions

HDL-associated enzymes such as PON1, Lp-PLA<sub>2</sub>, and LCAT function as antioxidants by reducing oxidized lipids. To determine the antioxidant properties of the HDL subfractions, we examined the relative amount of PON1, Lp-PLA<sub>2</sub>, and LCAT protein in each subfraction by using Western blot analysis. PON1 was observed in H4 and H5 but was markedly more abundant in H5 than in H4 (Figure 4A). Lp-PLA<sub>2</sub>, which produces lyso-phospholipids and free fatty acids by hydrolyzing the sn-2 group of phospholipids in lipoproteins and cell membranes, was most abundant in H4 (Figure 4A). LCAT, which is responsible for the synthesis of cholesteryl ester, was most abundant in H4 and H5. In addition, we determined the LCAT activity in each HDL subfraction, measured as the change in F<sub>470/390</sub> per minute (Figure 4B). LCAT activity was significantly higher in H4 and H5 than in any other subfraction, which coincided with the higher LCAT protein levels observed in these subfractions. Modifications of PON1, Lp-PLA<sub>2</sub>, and LCAT are rarely reported; however, the activity level of these enzymes has been found to be significantly reduced in modified HDL and different disease states.<sup>53-54</sup>

### Relative Quantification of Proteins in HDL Subfractions by Using iTRAQ Labeling and NanoLC-MS/MS

Recently, MS technology has been used to show the proteomic diversity of HDL.<sup>55</sup> To identify HDL-associated proteins, we used iTRAQ labeling and nanoLC-MS/MS,<sup>56</sup> a high-throughput, sensitive method for simultaneously identifying and quantifying proteins in biologic samples. We first used 4-plex iTRAQ reagents (mass tag 114, 115, 116, and 117) to label H1 through H4. We then used iTRAQ reagents (mass tag 114 and 117) to label H3 and H5, respectively. By combining data from the 2 experiments, we obtained the protein ratios of H1 through H5 and identified 88 HDL-associated proteins (Table S-1, Supporting Information).

The proteins detected in HDL were classified on the basis of molecular function by using gene ontology analysis (Table S-2, Supporting Information). Classification categories included lipid metabolism, antioxidation, acute-phase response, complement, protease inhibitor, and immune response. The diversity of these annotations relates to the multifunctionality of HDL. In addition, most of the proteins detected have more than 1 function. Different colors were used to indicate the relative abundance of each protein: green (low), yellow (medium), and red (high). Important HDL-associated enzymes, such as phospholipid transfer protein (PLTP), LCAT, Lp-PLA<sub>2</sub>, PON1 and PON3, were most abundant in the more negatively charged subfractions (H4 and/or H5). Acute-phase proteins were dominantly associated with the more negatively charged HDL subfractions, although SAA1 and SAA4 were most abundant in H1 and H2. The concentrations of acute-phase proteins are markedly altered in response to infection, injury, or inflammation.<sup>57</sup> All of the acute-phase proteins found in HDL increase during inflammation except transthyretin, which decreases.<sup>57</sup> The complement proteins (clusterin, C4A, and vitronectin) were most abundant in H3 through H5. Four protease inhibitors (alpha-1-antitrypsin, alpha-2-antiplasmin, antithrombin-III, and angiotensinogen) were also most abundant in H3 through



H5. The antioxidant enzymes (LCAT, Lp-PLA<sub>2</sub>, PON1, PON3, apoAI, and apoM) were more abundant in H4 and H5 than in H1 through H3, which is consistent with our Western blot data for LCAT, Lp-PLA<sub>2</sub>, and PON1, suggesting that H4 and H5 may be the most antioxidant-rich HDL subfractions.

### Antioxidant Activity of HDL Subfractions

To estimate the antioxidant activity of HDL subfractions, we examined the effect of each subfraction on LDL peroxidation over time by measuring the formation of conjugated dienes from the unsaturated fatty acids of LDL (Figure 5A). In these experiments, AAPH was used to generate organic free radicals to induce LDL peroxidation in the presence of each HDL subfraction. We found that H1 had the fastest propagation rate of all the subfractions, indicating that it had the lowest antioxidant activity (Figure 5A). In addition, by comparing the maximum propagation rates of subfractions H2 through H5 to that of H1, we showed that the suppression of LDL oxidation increased with the increasing electronegativity of the HDL subfractions. Thus, H4 and H5 had the highest antioxidant activity among all of the HDL subfractions (Figure 5B), which is consistent with our nanoLC MS/MS results.

### Effects of HDL Subfractions on Cholesterol Efflux

The HDL-induced efflux of cholesterol from lipid-laden macrophages helps to prevent atherosclerosis. To determine the effects of HDL subfractions on cholesterol efflux, we performed quantitative cholesterol efflux assays with 22-NBD-cholesterol, which is a fluorescently labeled analog of cholesterol that has been used for tracing cholesterol uptake.<sup>58</sup> Previously, HDL was shown to stimulate cholesterol efflux from mouse macrophage RAW 264.7 cells.<sup>59</sup> Using these same cells in our cholesterol efflux experiments, we found that HDL subfractions with increasing electronegativity increased cholesterol efflux from macrophages, with the exception of H5, which promoted the least amount of cholesterol efflux (Figure 6).

In our study, H5 had the highest level of PON1 but the weakest ability to induce cholesterol efflux. Therefore, the ability of H5 to induce cholesterol efflux may be affected by other enzymes or protein modifications. The weak induction of cholesterol efflux by H5 may be attributed to the presence of the highly negatively charged isoforms of apoAI and apoCIII. For example, oxidized apoAI has an impaired cholesterol efflux ability because it is unable to activate LCAT or bind to ATP-binding cassette transporter A1 (ABCA1), a macrophage cholesterol exporter.<sup>60</sup> Recently, other researchers reported that glycated apoAI also has an impaired cholesterol efflux ability.<sup>61</sup> Glycation of apoAI decreases the stability of lipid-apolipoprotein interactions and apolipoprotein self-association, which affects the structural cohesion of HDL particles.<sup>62</sup> Notably, high levels of glycated apoAI have been found in diabetic and nephropathic patients.<sup>37</sup> When the apoAI in HDL becomes modified, it may lose its protective effect or become pro-atherogenic. ApoCIII, which we found most abundantly in H5, could influence the cholesterol efflux function by reducing the proportion of apoAI in HDL.<sup>63-64</sup> The fact that H5 showed the highest esterification activity but the lowest efflux activity may further prove that LCAT esterification is independent of cholesterol efflux ability. These findings have also been reported in other studies.<sup>65-66</sup>

## CONCLUSIONS

We have established a novel technique for the fractionation of HDL by using anion-exchange chromatography to study the compositional and functional heterogeneity of HDL. Because ultracentrifugation and anion-exchange chromatography are different purification techniques, subfractions obtained by using density-gradient ultracentrifugation are expected to be different from charge-defined subfractions obtained by using anion-exchange

chromatography. HDL2 and HDL3 separated by using density-gradient ultracentrifugation have been shown to differ in the percentages of lipid and protein.<sup>15</sup> We found that H1-H5 separated by using anion-exchange chromatography have similar percentages of lipid and protein but differ significantly in their protein components. Changes in the protein composition of HDL have been reported to decrease its atheroprotective activity.<sup>67-68</sup> Therefore, this approach could be used to determine which HDL-associated enzymes and proteins play important roles in diseases such as atherosclerosis by comparing the relative expression and activity levels of HDL components in subfractions from healthy individuals and patients with different diseases. In turn, this may lead to the discovery of new pharmacologic targets for preventing atherogenesis. Future research in our lab will focus on characterizing the HDL subfractions from patients with type II diabetes and uremia.

## Supplementary Material

Refer to Web version on PubMed Central for supplementary material.

## Acknowledgments

This work was supported by grants from the National Institutes of Health (HL63364); the American Diabetes Association (7-03-RA-108, CYY; 1-04-RA-13, CHC); the National Science Council (NSC 101-2113-M-039-002-MY2, NSC 100-2314-B-039-040-MY3); Academia Sinica (BM102021169); and the Taiwan Department of Health, Clinical Trial, Research Center of Excellence (DOH102-TD-B-111-004), and the Roderick D. MacDonald Research Fund, Texas, USA.

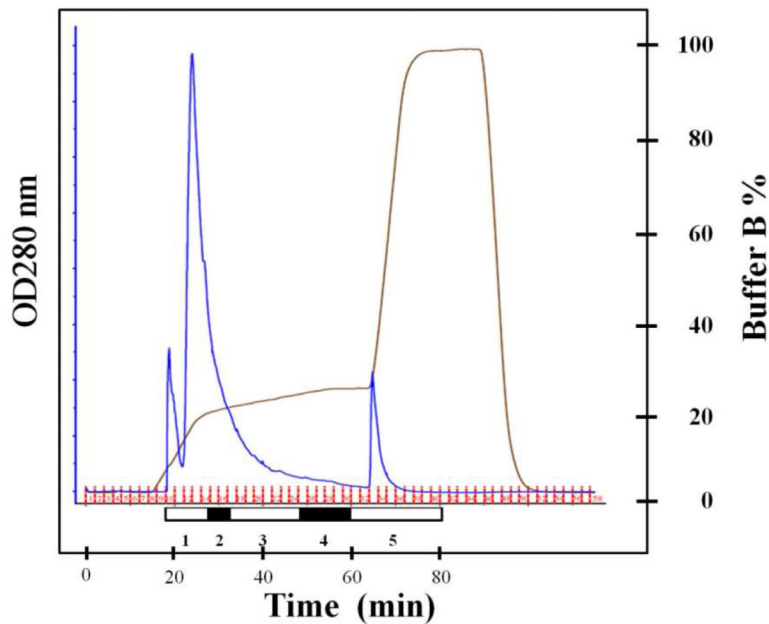
## REFERENCES

1. Castelli WP, Garrison RJ, Wilson PW, Abbott RD, Kalousdian S, Kannel WB. JAMA. 1986; 256:2835–2838. [PubMed: 3773200]
2. Gordon DJ, Rifkind BM. N. Engl. J. Med. 1989; 321:1311–1316. [PubMed: 2677733]
3. Chapman MJ, Assmann G, Fruchart JC, Shepherd J, Sirtori C. Curr. Med. Res. Opin. 2004; 20:1253–1268. [PubMed: 15324528]
4. Kontush A, Chapman MJ. Nat Clin Pract Cardiovasc Med. 2006; 3:144–153. [PubMed: 16505860]
5. Van Lenten BJ, Hama SY, de Beer FC, Stafforini DM, McIntyre TM, Prescott SM, La Du BN, Fogelman AM, Navab M. J. Clin. Invest. 1995; 96:2758–2767. [PubMed: 8675645]
6. Vaisar T, Pennathur S, Green PS, Gharib SA, Hoofnagle AN, Cheung MC, Byun J, Vuletic S, Kassim S, Singh P, Chea H, Knopp RH, Brunzell J, Geary R, Chait A, Zhao XQ, Elkon K, Marcovina S, Ridker P, Oram JF, Heinecke JW. J. Clin. Invest. 2007; 117:746–756. [PubMed: 17332893]
7. O'Connell BJ, Genest J, Jr. Circulation. 2001; 104:1978–1983. [PubMed: 11602504]
8. Movva R, Rader DJ. Clin. Chem. 2008; 54:788–800. [PubMed: 18375481]
9. Tall AR. J. Intern. Med. 2008; 263:256–273. [PubMed: 18271871]
10. Nofer JR, Levkau B, Wolinska I, Junker R, Fobker M, von Eckardstein A, Seedorf U, Assmann G. J. Biol. Chem. 2001; 276:34480–34485. [PubMed: 11432865]
11. Barter PJ, Nicholls S, Rye KA, Anantharamaiah GM, Navab M, Fogelman AM. Circ. Res. 2004; 95:764–772. [PubMed: 15486323]
12. Gofman JW, Young W, Tandy R. Circulation. 1966; 34:679–697. [PubMed: 5921763]
13. Pownall HJ, Van Winkle WB, Pao Q, Rohde M, Gotto AM Jr. Biochim. Biophys. Acta. 1982; 713:494–503. [PubMed: 6817809]
14. Salonen JT, Salonen R, Seppanen K, Rauramaa R, Tuomilehto J. Circulation. 1991; 84:129–139. [PubMed: 2060089]
15. Kontush A, Chantepie S, Chapman MJ. Arterioscler. Thromb. Vasc. Biol. 2003; 23:1881–1888. [PubMed: 12920049]
16. Cheung MC, Albers JJ. J. Biol. Chem. 1984; 259:12201–12209. [PubMed: 6434538]

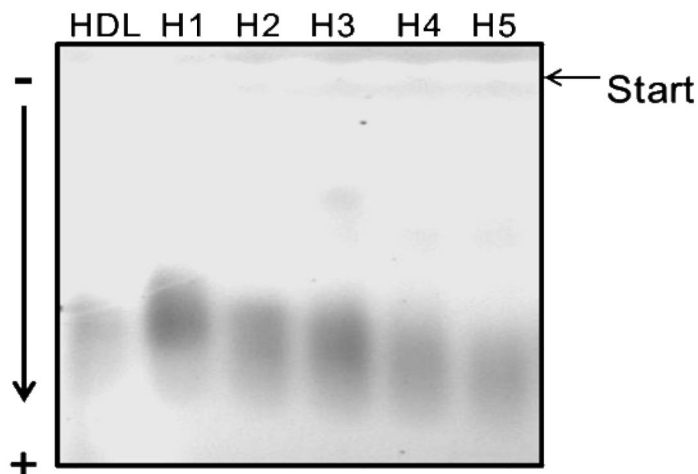
17. Koren E, Puchois P, Alaupovic P, Fesmire J, Kandoussi A, Fruchart JC. *Clin. Chem.* 1987; 33:38–43. [PubMed: 3100097]
18. Jeyarajah EJ, Cromwell WC, Otvos JD. *Clin. Lab. Med.* 2006; 26:847–870. [PubMed: 17110242]
19. Asztalos BF, Sloop CH, Wong L, Roheim PS. *Biochim. Biophys. Acta.* 1993; 1169:291–300. [PubMed: 7548123]
20. Kurosawa H, Yoshida H, Yanai H, Ogura Y, Hirowatari Y, Tada N. *Clin. Biochem.* 2007; 40:1291–1296. [PubMed: 17826753]
21. Ott GS, Shore VG. *J. Chromatogr.* 1982; 231:1–12. [PubMed: 7119051]
22. Hirowatari Y, Yoshida H, Kurosawa H, Doumitu KI, Tada N. *J. Lipid Res.* 2003; 44:1404–1412. [PubMed: 12730306]
23. Rubenstein B. *Atherosclerosis.* 1979; 33:415–423. [PubMed: 228680]
24. Hirowatari Y, Tsunoda Y, Ogura Y, Homma Y. *Atherosclerosis.* 2009; 204:e52–57. [PubMed: 19091316]
25. Yang CY, Raya JL, Chen HH, Chen CH, Abe Y, Pownall HJ, Taylor AA, Smith CV. *Arterioscler. Thromb. Vasc. Biol.* 2003; 23:1083–1090. [PubMed: 12689919]
26. Yang CY, Chen HH, Huang MT, Raya JL, Yang JH, Chen CH, Gaubatz JW, Pownall HJ, Taylor AA, Ballantyne CM, Jenniskens FA, Smith CV. *Atherosclerosis.* 2007; 193:283–291. [PubMed: 17030034]
27. *JAMA.* 2001; 285:2486–2497. [PubMed: 11368702]
28. Havel RJ, Eder HA, Bragdon JH. *J. Clin. Invest.* 1955; 34:1345–1353. [PubMed: 13252080]
29. Smith PK, Krohn RI, Hermanson GT, Mallia AK, Gartner FH, Provenzano MD, Fujimoto EK, Goetze NM, Olson BJ, Klenk DC. *Anal. Biochem.* 1985; 150:76–85. [PubMed: 3843705]
30. Chen CJ, Lai CC, Tseng MC, Liu YC, Lin SY, Tsai FJ. *Anal. Chim. Acta.* 2013; 783:31–38. [PubMed: 23726097]
31. Cominacini L, Garbin U, Davoli A, Micciolo R, Bosello O, Gaviraghi G, Scuro LA, Pastorino AM. *J. Lipid Res.* 1991; 32:349–358. [PubMed: 2066667]
32. Sankaranarayanan S, Kellner-Weibel G, de la Llera-Moya M, Phillips MC, Asztalos BF, Bittman R, Rothblat GH. *J. Lipid Res.* 2011; 52:2332–2340. [PubMed: 21957199]
33. Rosenblat M, Vaya J, Shih D, Aviram M. *Atherosclerosis.* 2005; 179:69–77. [PubMed: 15721011]
34. Noto H, Hara M, Karasawa K, Iso ON, Satoh H, Togo M, Hashimoto Y, Yamada Y, Kosaka T, Kawamura M, Kimura S, Tsukamoto K. *Arterioscler. Thromb. Vasc. Biol.* 2003; 23:829–835. [PubMed: 12649088]
35. Garner B, Waldeck AR, Witting PK, Rye KA, Stocker R. *J. Biol. Chem.* 1998; 273:6088–6095. [PubMed: 9497326]
36. Jaleel A, Henderson GC, Madden BJ, Klaus KA, Morse DM, Gopala S, Nair KS. *Diabetes.* 2010; 59:2366–2374. [PubMed: 20622162]
37. Lapolla A, Brioschi M, Banfi C, Tremoli E, Bonfante L, Cristoni S, Seraglia R, Traldi P. *J. Mass Spectrom.* 2008; 43:74–81. [PubMed: 17721906]
38. Brown WV. *J Clin Lipidol.* 2007; 1:7–19. [PubMed: 21291664]
39. Young EK, Chatterjee C, Sparks DL. *Am. J. Pathol.* 2009; 175:448–457. [PubMed: 19528346]
40. Bondarenko PV, Farwig ZN, McNeal CJ, Macfarlane RD. *International Journal of Mass Spectrometry.* 2002; 219:671–680.
41. Jong MC, Hofker MH, Havekes LM. *Arterioscler. Thromb. Vasc. Biol.* 1999; 19:472–484. [PubMed: 10073946]
42. Bondarenko PV, Cockrill SL, Watkins LK, Cruzado ID, Macfarlane RD. *J. Lipid Res.* 1999; 40:543–555. [PubMed: 10064743]
43. Meneilly GS, Demuth HU, McIntosh CH, Pederson RA. *Diabet. Med.* 2000; 17:346–350. [PubMed: 10872532]
44. Vaisar T, Mayer P, Nilsson E, Zhao XQ, Knopp R, Prazen BJ. *Clin. Chim. Acta.* 2010; 411:972–979. [PubMed: 20307520]
45. Chang CT, Liao HY, Chang CM, Chen CY, Chen CH, Yang CY, Tsai FJ, Chen CJ. *Clin. Chim. Acta.* 2013; 420:69–75. [PubMed: 23078847]

46. Ito Y, Breslow JL, Chait BT. *J. Lipid Res.* 1989; 30:1781–1787. [PubMed: 2614277]
47. Kowal RC, Herz J, Weisgraber KH, Mahley RW, Brown MS, Goldstein JL. *J. Biol. Chem.* 1990; 265:10771–10779. [PubMed: 2355022]
48. Sehayek E, Eisenberg S. *J. Biol. Chem.* 1991; 266:18259–18267. [PubMed: 1917954]
49. Ooi EM, Barrett PH, Chan DC, Watts GF. *Clin Sci (Lond).* 2008; 114:611–624. [PubMed: 18399797]
50. Kinnunen PK, Ehnolm C. *FEBS Lett.* 1976; 65:354–357. [PubMed: 182536]
51. Kiernan UA, Tubbs KA, Nedelkov D, Niederkofler EE, Nelson RW. *FEBS Lett.* 2003; 537:166–170. [PubMed: 12606051]
52. Farwig ZN, McNeal CJ, Little D, Baisden CE, Macfarlane RD. *Biochem. Biophys. Res. Commun.* 2005; 332:352–356. [PubMed: 15910745]
53. Ferretti G, Bacchetti T, Marchionni C, Caldarelli L, Curatola G. *Acta Diabetol.* 2001; 38:163–169. [PubMed: 11855794]
54. Fournier N, Myara I, Atger V, Moatti N. *Clin. Chim. Acta.* 1995; 234:47–61. [PubMed: 7758222]
55. Shah AS, Tan L, Lu Long J, Davidson WS. *J. Lipid Res.* 2013; 54:2575–2585. [PubMed: 23434634]
56. Chen CJ, Chen WY, Tseng MC, Chen YR. *Anal. Chem.* 2012; 84:297–303. [PubMed: 22097963]
57. Gabay C, Kushner IN. *Engl. J. Med.* 1999; 340:448–454.
58. Frolov A, Petrescu A, Atshaves BP, So PT, Gratton E, Serrero G, Schroeder F. *J. Biol. Chem.* 2000; 275:12769–12780. [PubMed: 10777574]
59. Toledo JD, Cabaleiro LV, Garda HA, Gonzalez MC. *J. Cell. Biochem.* 2011; 54:2575–2585.
60. Shao B, Oda MN, Oram JF, Heinecke JW. *Chem. Res. Toxicol.* 2010; 23:447–454. [PubMed: 20043647]
61. Hoang A, Murphy AJ, Coughlan MT, Thomas MC, Forbes JM, O'Brien R, Cooper ME, Chindusting JP, Sviridov D. *Diabetologia.* 2007; 50:1770–1779. [PubMed: 17579831]
62. Calvo C, Talussot C, Ponsin G, Berthezene F. *Biochem. Biophys. Res. Commun.* 1988; 153:1060–1067. [PubMed: 3134018]
63. Hara H, Yokoyama S. *J. Biol. Chem.* 1991; 266:3080–3086. [PubMed: 1993681]
64. Holzer M, Birner-Gruenberger R, Stojakovic T, El-Gamal D, Binder V, Wadsack C, Heinemann A, Marsche G. *J. Am. Soc. Nephrol.* 2011; 22:1631–1641. [PubMed: 21804091]
65. Kilsdonk EP, Dorsman AN, van Tol A. *Int. J. Biochem.* 1993; 25:219–221. [PubMed: 8444318]
66. Tanigawa H, Billheimer JT, Tohyama J, Fuki IV, Ng DS, Rothblat GH, Rader DJ. *Circulation.* 2009; 120:160–169. [PubMed: 19564558]
67. G HB, Rao VS, Kakkar VV. *Cholesterol.* 2011; 2011:274629. [PubMed: 21490770]
68. Smith JD. *Arterioscler. Thromb. Vasc. Biol.* 2010; 30:151–155. [PubMed: 19679832]

(A)



(B)

**Figure 1.**

Separation of HDL into 5 distinct subfractions according to charge. (A) FPLC elution profiles of the 5 HDL subfractions separated by using a UnoQ12 column and the Tris-HCl buffer system at a flow rate of 2 mL/minute. Approximately 100 mg of HDL in 10 mL was loaded onto the column and separated with a multistep gradient of buffer B. Elution was monitored at 280 nm. (B) Results of agarose gel electrophoresis of HDL and subfractions H1 through H5. Each HDL sample (2.5  $\mu$ g in 9  $\mu$ L) was loaded onto a 0.7% agarose gel and separated at 100 V for 1.4 hours.



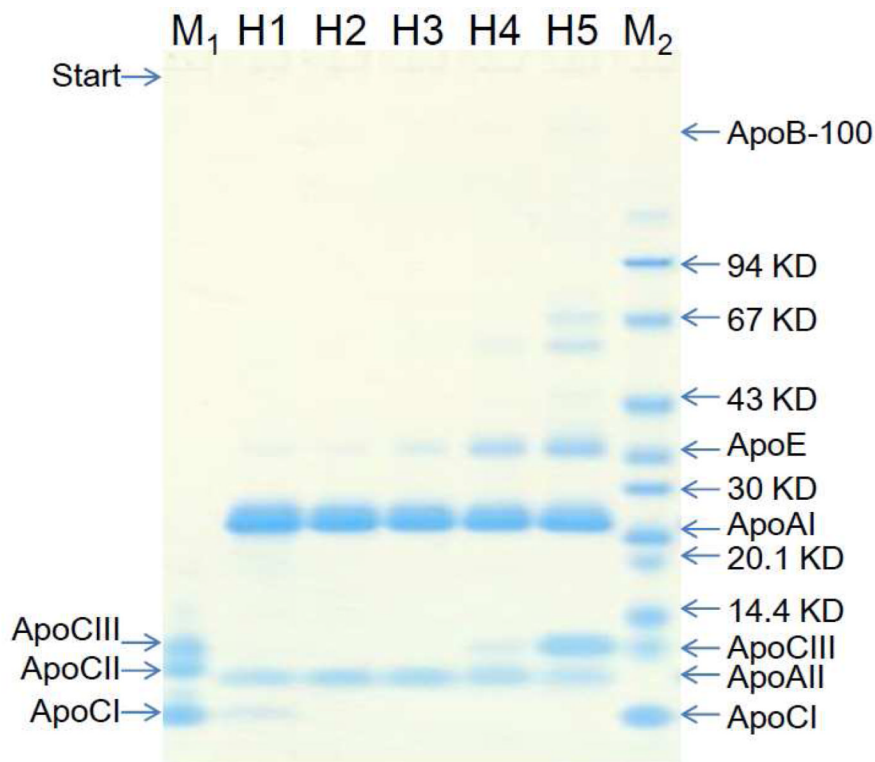


**Figure 2.** SDS-PAGE analyses of HDL subfractions. Approximately 3  $\mu$ g of each HDL subfraction or the indicated reference standard was loaded and separated on a linear gradient Bis-Tris 4% to 12% gel at 135 V for 65 min. The gels were stained for 1 hour in SimplyBlue and destained in water. Bands were identified by comparisons with known protein standards. M<sub>1</sub>, human ApoCs standard; M<sub>2</sub>, human apolipoprotein mix2 standard.

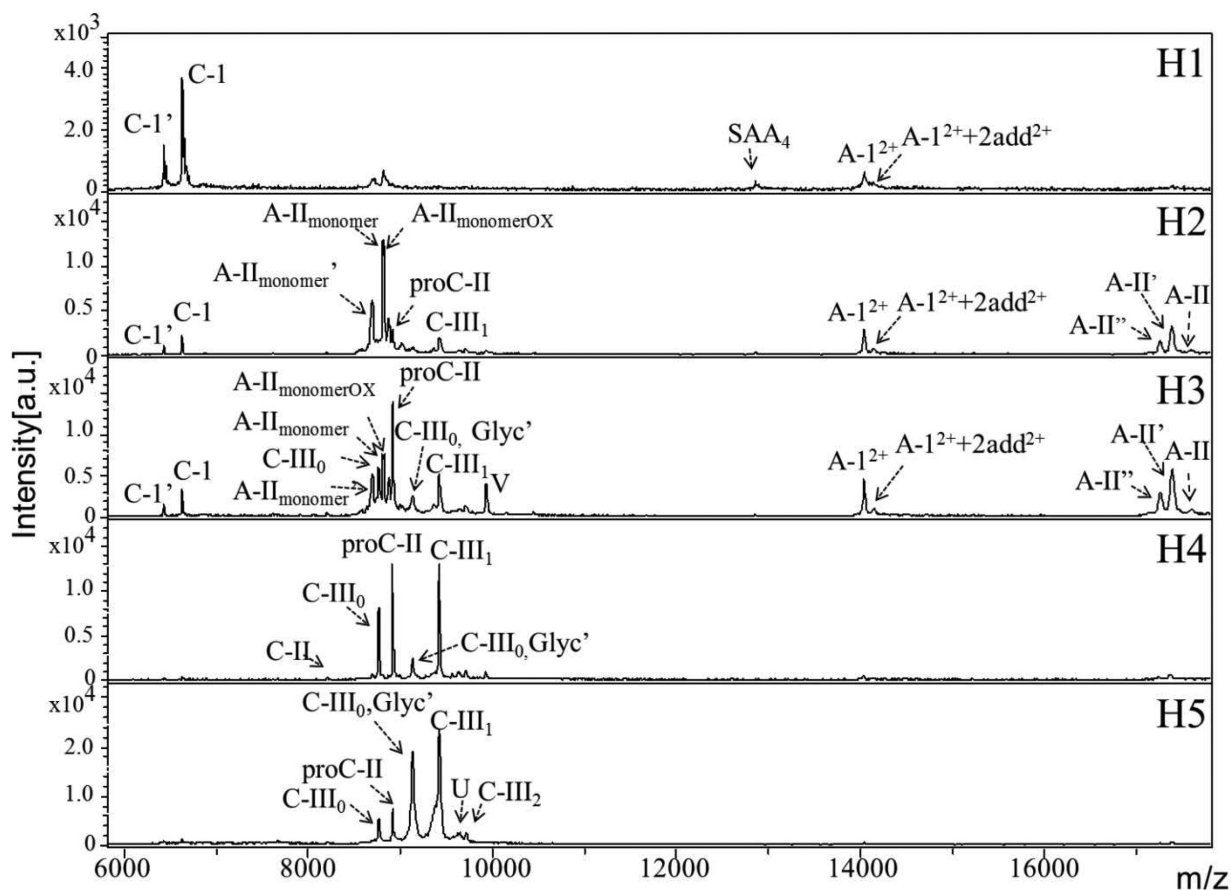
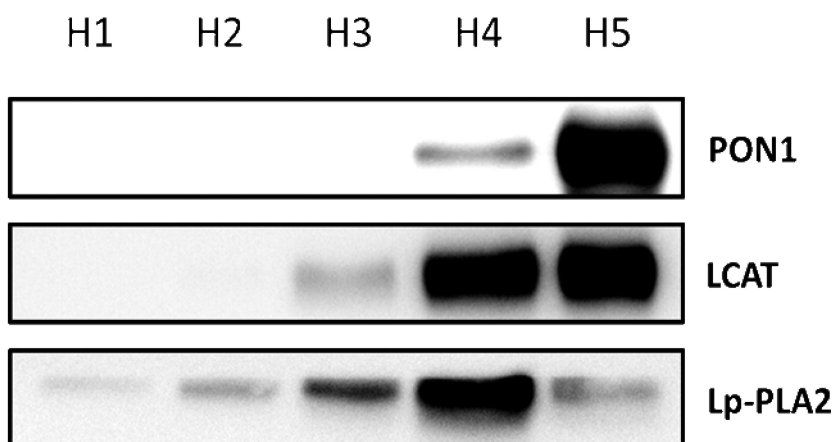


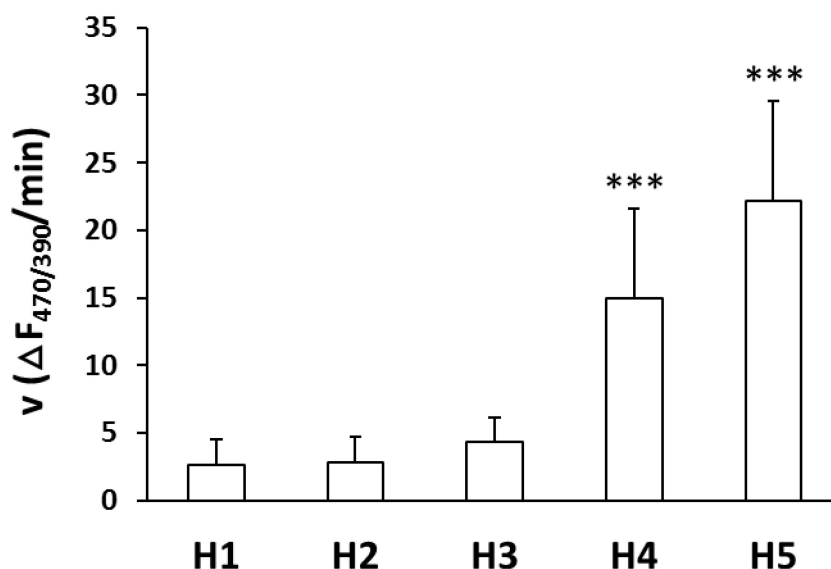
**Figure 3.**

MALDI-TOF-MS analysis of HDL subfractions. MALDI-TOF-MS analysis was performed to identify the major apolipoproteins and their isoforms in each HDL subfraction. The MS peaks for H1 through H5 are shown. A-1, apoAI (calculated mass: 28078 m/z); A-1<sup>2+</sup>+2add<sup>2+</sup>, apoAI+ two 98-Da adducts (calculated mass: 14137.4 m/z); A-II, apoAII (calculated mass: 17379.8 m/z); A-II', apoAII minus C-terminus-Gln (calculated mass: 17253.7 m/z); A-II'', apoAII minus two C-terminus-Gln (calculated mass: 17125.6 m/z); A-II<sub>monomer</sub>, single chain apoAII (calculated mass: 8809.9 m/z); A-II<sub>monomer</sub>', single chain apoAII minus C-terminus-Gln (calculated mass: 8581.8 m/z); A-II<sub>monomer</sub>ox, oxidized single chain apoAII (calculated mass: 8825.9 m/z); C-1, apoCI (calculated mass: 6630.6 m/z); C-1', apoCI minus N-terminus Thr-Pro (calculated mass: 6432.4 m/z); C-II, apoCII (calculated mass: 8204.1 m/z); proC-II, pro-apoCII (calculated mass: 8914.9 m/z); C-III<sub>0</sub>, apoCIII<sub>0</sub> (calculated mass: 8765.7 m/z); C-III<sub>1</sub>, apoCIII<sub>1</sub> (calculated mass: 9421.3 m/z); C-III<sub>0</sub>Glyc', Galβ1, 3GalNAc-O-apoCIII<sub>0</sub> (calculated mass: 9130.0 m/z); U, apoCIII<sub>1</sub>+206-Da adduct (calculated mass: 9627.5 m/z); V, apoCIII<sub>2</sub>+221-Da isoform (calculated mass: 9933.6 m/z).

(A)



(B)

**Figure 4.**

Analysis of antioxidant enzymes in HDL subfractions. (A) Western blot analysis showing the relative amount of LCAT, PON1, and Lp-PLA<sub>2</sub> in each HDL subfraction. A 7% acrylamide gel was used for the analysis of LCAT and PON1 proteins (7.5  $\mu\text{g}/\text{well}$ ), and a 12% acrylamide gel was used for the analysis of Lp-PLA<sub>2</sub> protein (35  $\mu\text{g}/\text{well}$ ) (n=4). (B) The hydrolytic LCAT enzyme activity of each HDL subfraction, expressed as the change in fluorescence intensity at 470 nm/390 nm per minute. HDL subfractions (10  $\mu\text{g}$ ) were incubated with a fluorescent substrate at 37°C. Values shown are mean  $\pm$  SD and were compared by using one-way ANOVA with the Student-Newman-Keuls post hoc test.\*\*\* $P < 0.001$  vs H1, H2, and H3 (n=6).

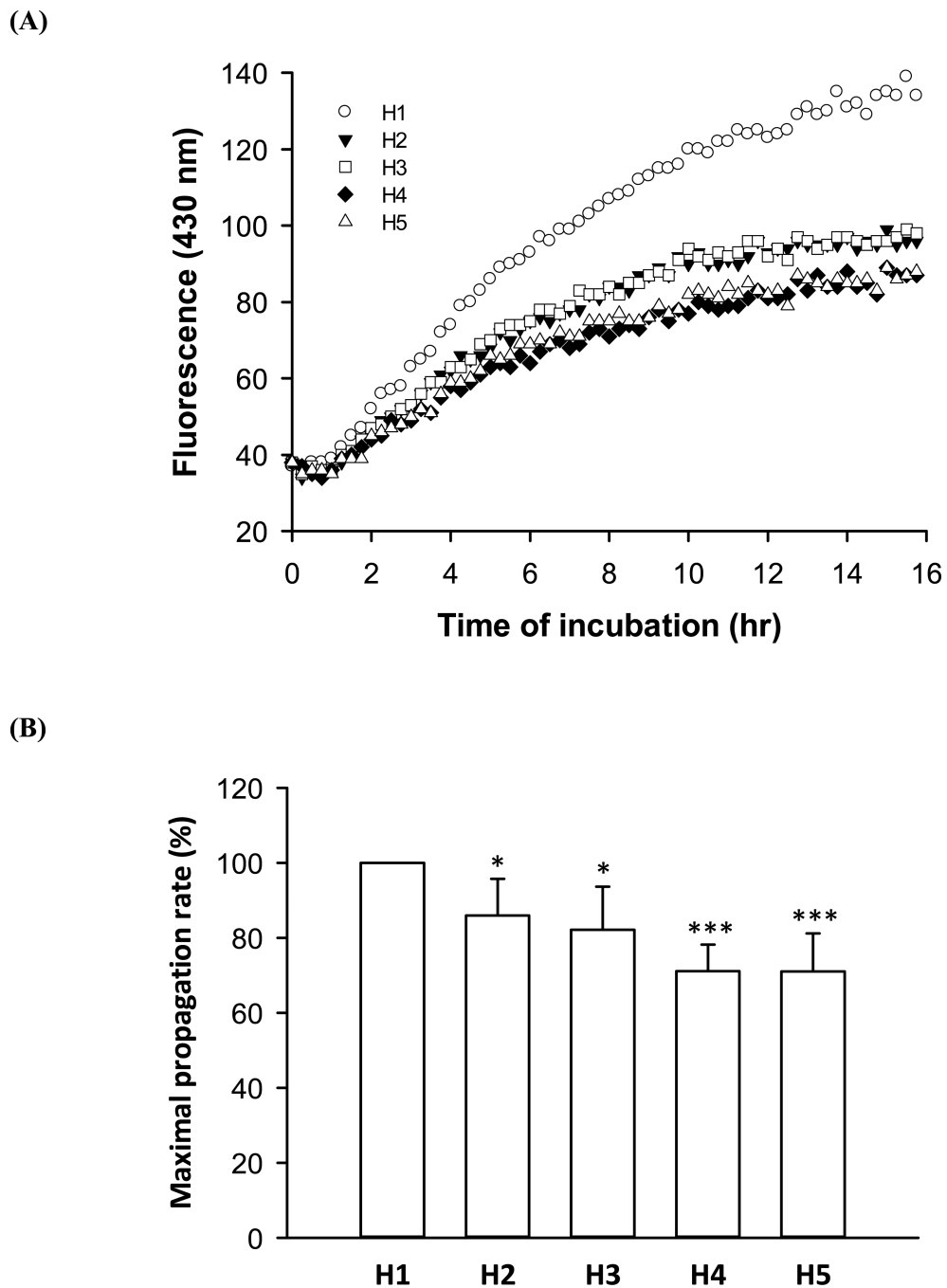


**Figure 5.** Antioxidant activity of HDL subfractions. (A) LDL (20  $\mu$ g) was incubated with HDL (40  $\mu$ g) and 10 mM AAPH at 37°C. The fluorescence (emission at 430 nm) produced by AAPH-induced lipid peroxidation was measured to determine the antioxidant activity of each HDL subfraction. (B) The maximum propagation rate of each subfraction was compared to that of H1. Values shown are mean  $\pm$  SD and were compared by using one-way ANOVA with the Student-Newman-Keuls post hoc test. \* $P$ <0.05 vs H1 and \*\*\* $P$ <0.001 vs H1 (n=5).

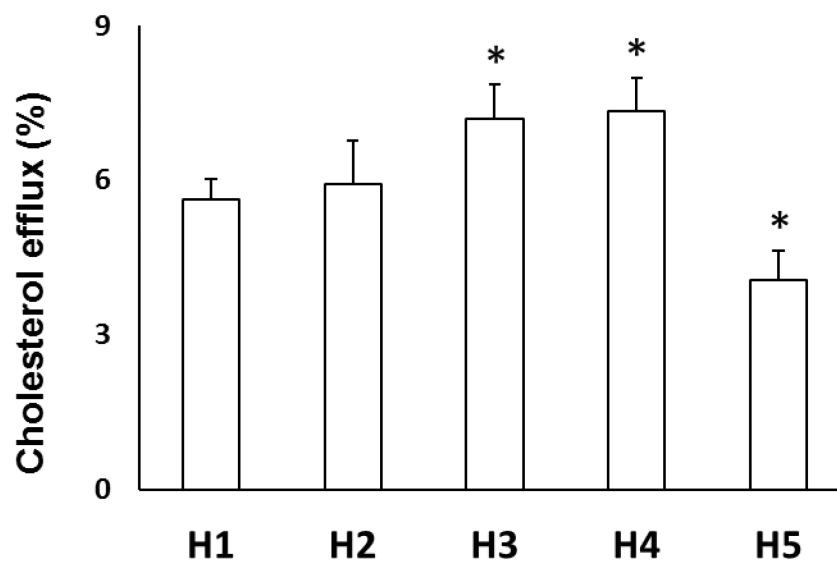


**Figure 6.** Effect of HDL subfractions on cholesterol efflux. RAW 264.7 cells were labeled with 10  $\mu\text{g}$  22-NBD-cholesterol, equilibrated with 0.2% bovine serum albumin, and incubated with each HDL subfraction, H1 through H5 (20  $\mu\text{g}$  each). Fluorescence was detected in an aliquot of medium. Values shown are the mean  $\pm$  SD. Each sample was measured in triplicate, and the cholesterol efflux ability of each subfraction was compared to that of H1 by using a Student *t*-test. \* $P < 0.01$  (n=4).



**Table 1**

Chemical Composition of HDL Subfractions H1 through H5 Obtained From Healthy Normolipidemic Donors (n=6)

Subfraction	Fraction Distribution (%)	Total Protein (%)	PL (%)	TG (%)	FC (%)	CE (%)	TC (%)
H1	59.9 ± 2.5	54.1 ± 6.9	23.5 ± 4.7	2.9 ± 2.2	3.2 ± 1.5	16.3 ± 3.7	19.5 ± 4.9
H2	13.1 ± 1.4	58.5 ± 3.8	20.9 ± 2.8	1.9 ± 0.6	2.3 ± 0.7	16.4 ± 2.9	18.7 ± 3.6
H3	15.5 ± 1.5	57.2 ± 2.5	18.4 ± 1.4	6.4 ± 3.6	0.9 ± 0.7 <sup>a</sup>	17.1 ± 3.1	18.0 ± 3.6
H4	3.8 ± 0.4	56.9 ± 4.5	20.5 ± 4.5	7.4 ± 4.1 <sup>b</sup>	1.2 ± 1.3 <sup>a</sup>	14.1 ± 2.1	15.2 ± 3.2
H5	7.7 ± 1.0	55.8 ± 6.9	17.3 ± 6.7	8.5 ± 4.6 <sup>a,b</sup>	2.3 ± 1.8	16.1 ± 2.5	18.4 ± 4.2

Data expressed as mean ± SD. PL, phospholipids; TG, triglycerides; FC, free cholesterol; CE, cholesteryl ester; TC, total cholesterol. The distributions of fraction components were compared by using one-way analysis of variance with the Student-Newman-Keuls post hoc test.

<sup>a</sup>  $P < 0.05$  vs H1

<sup>b</sup>  $P < 0.05$  vs H2. The percentage of total protein, PL, TG, and TC was determined by dividing each respective amount by the total combined amount in each subfraction. Thus, the sum of the percentages of total protein, PL, TG, and TC add up to 100%. TC (%) is equal to the sum of FC (%) and CE (%). The fraction distribution represents the integrated area of each subfraction on fast protein liquid chromatography divided by that of all fractions.